A Root Locus-Based Flutter Synthesis Procedure

Prabhat Hajela*
Stanford University, Stanford, California

An efficient generalized constraint is proposed in the context of a nonlinear mathematical programming approach for the minimum weight design of wing structures for flutter considerations. The approach is based on a root locus analysis procedure that is better suited for flutter redesign than the conventionally used *V-g* method. The proposed flutter constraint does not require an actual computation of the flutter speed, allows prescription of meaningful margins of safety in the optimized design, and lends itself to elegant computation of sensitivity information. The approach is implemented and results presented for representative structural models.

Nomenclature

$[\hat{A}]$ = generalized aerodynamics matrix
b = semichord of wing measured normal to the elastic axis
b_{ref} = reference value of the wing semichord
$[B]$ = aeroelastic matrix
$C(s)$ = Theodorsen function
$[C]$ = structural damping matrix
d = vector of design variables
g = measure of net damping in the structure
g_j = jth inequality constraint on response quantiy
k = reduced-frequency parameter
$[\hat{K}]$ = generalized stiffness matrix
$[\hat{M}]$ = generalized mass matrix
q = dynamic pressure parameter
$\bar{s}$ = nondimensional Laplace variable
$\{v\}$ = adjoint eigenvector of aeroelastic matrix
V = freestream velocity
V_{req} = reference freestream velocity below which flutter is to be excluded
W = objective function
$\{x\}$ = vector of nodal displacements
$\{z\}$ = vector of generalized displacements
γ_j = viscous damping ratio for the jth complex root
γ_{ref} = lower bound on the viscous damping ratio
η = real part of s
$[\lambda]$ = eigenvalues of the aeroelastic matrix
Λ = sweep angle for the elastic axis
ρ_a = air density
τ = imaginary part of s
ω_d = damped frequency of aeroelastic response
ω_{ref} = lower bound on the damped frequency

Introduction

WITH the development of lightweight, high-performance aircraft, it has become increasingly important to account for dynamic response characteristics in a minimum weight airframe synthesis problem. This task is further complicated with the inclusion of aeroelastic considerations in the design process. The flutter constraint exhibits nonlinear characteristics with variations in structural component size. Moreover, the calculation of the flutter speed repetitively in an optimization procedure can be a computationally expensive task.

Received Dec. 1, 1982; presented as Paper 83-0063 at the AIAA 21st Aerospace Sciences Meeting, Reno, Nev., Jan. 10-13, 1983; revision received June 22, 1983.

*Research Associate. Presently Assistant Professor of Engineering Sciences, University of Florida. Member AIAA.

Perhaps the first flutter synthesis effort can be attributed to a 1969 effort of Turner.[1] Several research publications have focused on this subject since,[2-4] involving both the optimality criteria and the nonlinear programming methodology for optimization. With the ready availability of optimization algorithms and efficient discrete analysis programs, optimal flutter synthesis is not a conceptually difficult problem. However, with the emphasis on automated design capabilities, it is necessary to incorporate efficient flutter analysis procedures that would require minimal user interaction. Of the competing methods for aeroelastic stability analysis, the *V-g* method is perhaps the most extensively used. Despite the widespread application of this approach, there are some serious drawbacks that detract from its effectiveness. These drawbacks stem from the limitations of the *V-g* method and are briefly discussed in this paper. A better way of formulating the flutter constraint presents itself if the aeroelastic analysis were to be done by a root locus procedure.[5] This formulation is based on a cumulative constraint concept[6] that allows the user to fold multiple inequality constraints into a single representative measure. Additionally, the constraint gradients can be computed analytically in an efficient manner.

Problem Statement

The general nonlinear programming statement for the weight minimization problem can be written as

Minimize

$$W(d) \tag{1}$$

subject to

$$g_j(d) \le 0 \qquad j=1,2,\ldots,nr \tag{2}$$

and the side constraints on the design variables

$$d_i^l \le d_i \le d_i^u \qquad i=1,2,\ldots,n \tag{3}$$

where W is typically the weight of the structure; g_j the inequality constraints representing bounds on response quantities; and d_i^l and d_i^u the lower and upper bounds on the design variables, d_i, respectively. In the present formulation, g_j is the constraint needed to exclude flutter from the flight regime and the bounds on the design variables are specified from strength and displacement considerations.

Algorithms of mathematical nonlinear programming have proven invaluable in the optimal design of complex structural systems. However, the efficiency of these algorithms is seriously compromised in the presence of a large number of design variables and constraints. The basic idea of the cumulative constraint is to form a representative envelope of the multiple inequality constraints. This concept stems from looking at the constraints from a global structural viewpoint

rather than at the element component level. Three possible forms of the constraint have been proposed and evaluated in extensive detail.[7] The constraint that was implemented in the present work can be written as follows:

$$K = -\epsilon + \sum_{i=1}^{nr} \langle g_i \rangle^r \qquad \text{if } K > \psi$$

$$= -\epsilon + \frac{1}{\rho} Ln\left(\sum_{i=1}^{nr} \exp(\rho g_i) \right) \qquad \text{if } K \le \psi \tag{4}$$

where

$$\langle g_i \rangle = \begin{cases} g_i & \text{if } g_i > 0 \\ 0 & \text{if } g_i \le 0 \end{cases} \tag{5}$$

The above formulation folds the nr inequality constraints into the cumulative measure K. The constraint function K switches between two functional representations and this transition is governed by the preassigned numerical value of ψ, selected such that the transition occurs close to the constraint boundary. Factor ρ determines the relative participation of the individual constraints g_j in the cumulative measure and is typically of the order 10^2.

Flutter Optimization via *V*-g Method

This method of flutter analysis has been extensively used and referenced in literature.[8,9] A system is said to be critical in flutter if it undergoes steady-state oscillations without damping. If there is a net transfer of energy from the air to the structure, the amplitude of the oscillations increases in time, resulting in a divergent instability. Taking recourse to a modal approach to describe the response of the structure in terms of a finite number of degrees of freedom, the linearized flutter equation can be written as follows

$$(\Omega[\hat{K}] - [\hat{M}] - [\hat{A}(k)])\{z\} = 0 \tag{6}$$

where

$$[\hat{K}] = [\Phi]^T [K] [\Phi] \tag{7a}$$

$$[\hat{M}] = [\Phi]^T [M] [\Phi] \tag{7b}$$

$$\{z\} = -[\Phi]^T \{x\} \tag{7c}$$

In the above equations, $[\Phi]$ is the modal matrix and its columns typically contain coordinates of natural modes of vibration of the structure; $[\hat{K}]$ and $[\hat{M}]$ the generalized stiffness and mass matrices; $[\hat{A}]$ the generalized matrix of aerodynamic forces; x the vector of nodal displacements; and $\{z\}$ a vector of generalized displacements. The complex eigenvalue Ω is defined as follows:

$$\Omega = (1 + ig)/\omega^2$$

where ω is the frequency and g the damping parameter. For each value of the reduced frequency parameter $k = \omega b/V$, Eq. (6) is used to compute a set of complex eigenvalues Ω from which the corresponding set of V-g points can be calculated. These points are then mapped on a familiar V-g plot (Fig. 1) to obtain the V-g curve. A crossover of the $g = 0$ line in any mode indicates a flutter condition for that mode at the corresponding velocity (i.e., the damping parameter is zero). The optimization task can thus be stated as a redesign for minimum weight subject to the constraint that no mode has a crossover of the zero damping line at flight speeds less than a specified quantity. Despite the apparent advantages of this formulation that largely stem from an ease of analysis, there are some serious drawbacks that would suggest a search for an alternate procedure. These problem areas are linked to the following.

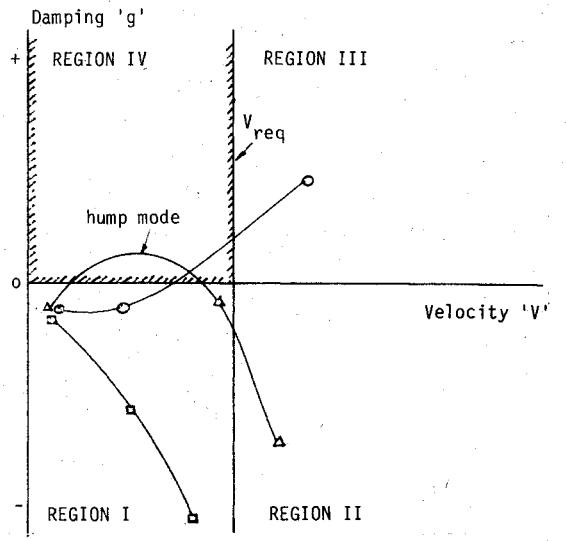

Fig. 1 Formulation of the generalized flutter constraint in the context of the *V*-*g* method for flutter synthesis.

1) The V-g plots are exclusively dependent on a somewhat ambiguous reduced frequency parameter k. When selecting a set of k values, it is not possible to predict the corresponding V-g value for a chosen mode. This can result in one of two problems: a) Chosen values of k may be such that the V-g pairs always lie in the quadrants I-III (Fig. 1), though the curve for a mode may have crossed the $g = 0$ line for $V < V_{req}$. In such a situation, the optimizer would not recognize a constraint violation. This was indeed the case for the wing box example considered here. An easy solution to this problem involves tracking the critical modes and linearly interpolating between crossover k values to determine the flutter speed. b) A hump mode-type instability[9] (Fig. 1) is hard to account for in an automated procedure and often requires a great deal of user interaction.

2) In the V-g approach, instability is described in terms of an artificial damping parameter g. This quantity is only meaningful for $g = 0$, that is, the state of undamped oscillatory response. Hence, it is not possible to formulate a constraint which prescribes a measure of viscous damping in the final design.

3) Third and perhaps not so critical is a different problem inherent with the V-g analysis procedure. The V-g plots for a given mode may "wind back," resulting in two damping constants for a single flight speed. This can provide misleading information to the optimizer and result in convergence problems.

Constraint Formulation in the *s* Plane

A root locus based aeroelastic stability analysis procedure provides a useful alternative method for formulating a flutter constraint that does not require the actual computation of the flutter speed. The equation of motion for the system can be written as

$$[M]\{\ddot{x}\} + [C]\{x\} + [K]\{x\} = \{Q_A(t)\} \tag{8}$$

where $[M]$, $[C]$, and $[K]$ are the mass, structural damping, and stiffness matrices; and $\{Q_A\}$ the vector of externally applied loads. In the present exercise, the structural damping is ignored although its inclusion does not entail any extensive effort. Writing the Laplace transform of Eq. (8) for zero initial conditions, one gets

$$\{[M]\bar{s}^2 + [K]\}\{X(\bar{s})\} = \{Q_A(\bar{s}, q)\} \tag{9}$$

where $q = \frac{1}{2}(\rho_a) V^2$ is the dynamic pressure and $\bar{s}$ the non-dimensional Laplace variable defined in terms of a reference

semichord b_{ref} and the quarter-chord sweep angle Λ as follows.

$$\bar{s}=\frac{sb_{ref}}{V\cos\Lambda} \tag{10}$$

Using the modal method of representation, Eq. (9) can be rewritten as

$$([\hat{M}]\bar{s}^2+[\hat{K}]-q[\hat{A}(\bar{s})])\{X(\bar{s})\}=0 \tag{11}$$

where $([\hat{M}]$ and $([\hat{K}]$ are the generalized mass and stiffness matrices as defined in Eq. (7); $[\hat{A}]$ is the generalized aerodynamics matrix and includes airloads due to the motion only; and $\{X(\bar{s})\}$ the vector of modal amplitudes. For various values of the dynamic pressure, q, the roots $\bar{s}$ that would yield a nontrivial solution to Eq. (11) are obtained from the characteristic equation

$$\det([\hat{M}]\bar{s}^2+[\hat{K}]-q[\hat{A}(\bar{s})])=0 \tag{12}$$

These roots are, in general, complex. The system would be unstable for that value of q for which one of the roots has a positive real part. The constraint can thus be formulated by choosing a set of dynamic pressures corresponding to flight speeds of interest, computing the roots of the characteristic equation (Eq. 12) and requiring that the real part be negative

$$g_j=Re(s_j)\le 0 \qquad j=1,2,\ldots,\ nr \tag{13}$$

$$nr=ndp\times nd$$

where nd is the order of the characteristic determinant and ndp the number of dynamic pressures considered. Since the root locus approach permits calculation of the viscous damping in each mode, the constraint can also be formulated such that the damping in a chosen mode be greater than a specified value. For a complex root

$$s_j=\eta_j+i\tau_j \tag{14}$$

the viscous damping ratio γ_j can be written as

$$\gamma_j=-\frac{\eta_j}{\sqrt{\eta_j^2+\tau_j^2}} \tag{15}$$

For such a constraint formulation it is also meaningful to restrict the damped frequency of the response at selected flight conditions to be greater than a specified value. A combination of the damping and frequency constraints results in the creation of the feasible and infeasible regions in the s-plane design space, as is illustrated in Fig. 2. It is important to keep the constraint value continuous when passing from one region to another.

Defining

$$X_s=\frac{\gamma}{\gamma_{ref}}-1 \tag{16}$$

$$Y_s=\frac{\omega_d}{\omega_{ref}}-1 \tag{17}$$

where

$$\omega_d=\sqrt{\eta_j^2+\tau_j^2} \tag{18}$$

γ_{ref} and ω_{ref} are the lower bounds on the viscous damping and the damped frequency, respectively. In addition to the nr constraints

$$Re(s_j)\le 0 \qquad j=1,2,\ldots,nr \tag{19}$$

the constraints in each of the four regions can be written as follows.

Region I:

$$g_i=-X_s\le 0 \tag{20}$$

Region II:

$$g_i=-\sqrt{X_s^2+Y_s^2}\le 0 \tag{21}$$

Region III:

$$g_i=-Y_s\le 0 \tag{22}$$

Region IV:

$$g_i=-\frac{X_s^2Y_s}{X_{sref}^2}-\frac{Y_s^2X_s}{Y_{sref}^2}\le 0 \tag{23}$$

where X_{sref} and Y_{sref} are typical values of X_s and Y_s encountered in region IV. This region is the inadmissible region as both the damping and frequency constraints are violated. The constraint formulation is peculiar in that two response parameters, γ and ω_d, are controlled by a change in the design variable vector. This is in contrast to say a stress constraint, where stress response alone is affected by a change in the design variable. The constraint violation in region IV can be alleviated by a move toward region I or upward into region III. It is therefore important that the constraint gradients in this region be structured so as to eliminate any bias toward a direction of move. Equations (20)-(23) were formulated with this objective in mind. These constraints can be folded into the cumulative measure K to yield a single inequality constraint for the problem. The proposed formulation is preferred over the V-g approach because it allows prescription of a realistic safety margin in the problem formulation. Moreover, the ambiguous reduced frequency parameter is replaced by a more meaningful dynamic pressure parameter for prescribing the flight conditions at which the stability analysis needs to be performed. Since the arrival and departure angles for roots at different dynamic pressures can be monitored in an automated procedure, it would be easier to detect hump mode-type instabilities.

Solution Procedure

The generalized mass and stiffness matrices were generated via a general purpose finite-element program. The natural modes of vibration for the structural model were also obtained in this program and were used to generate the elements of the matrix of generalized aerodynamic forces. Yates's modified strip theory aerodynamics[10] was used to determine the unsteady airloads. The presence of the transcendental

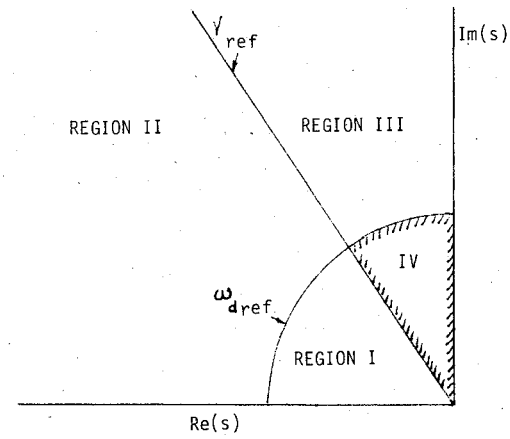

Fig. 2 Formulation of the generalized flutter constraint using a root locus approach.

function $C(\bar{s})$ tends to complicate the solution procedure. However, an approximation to this function proposed by R.T. Jones[11] simplifies the process. This approximation is written as a ratio of quadratic polynomials

$$C(\bar{s}) = C(\bar{s}) = \frac{c_1\bar{s}^2 + c_2\bar{s} + c_3}{d_i\bar{s}^2 + d_2\bar{s} + d_3} \tag{24}$$

$$\bar{s} = \frac{\bar{s}b_{\text{ref}}}{b} \tag{25}$$

where

$$c_1 = 0.5000 \qquad c_2 = 0.2808 \qquad c_3 = 0.01365$$

$$d_1 = 1.0000 \qquad d_2 = 0.3455 \qquad d_3 = 0.01365$$

For small values of the reduced frequency (0.1-0.5), this approximation has been demonstrated[12] to closely match the exact $C(\bar{s})$ function.

Constraint Gradients

Since the generation of constraint gradients via finite difference approximations requires a considerable investment of computational resource, it is important to be able to generate this information analytically. The constraint gradients require the calculation of quantities such as $\partial Re(s)/\partial d_j$ and $\partial Im(s)/\partial d_j$. Following an approach similar to the one proposed by Gwin and Taylor,[13] the properties of the adjoint eigenvalue problem can be exploited for this purpose. Equation (11) can be rewritten in the form

$$[B]\{X\} = 0 \tag{26}$$

where

$$[B] = ([\hat{M}]\bar{s}^2 + [\hat{K}] - q[\hat{A}]) \tag{27}$$

The adjoint eigenvalue problem can be written in terms of the adjoint eigenvector $\{v\}$ as

$$\{v\}^T[B] = 0 \tag{28}$$

Differentiating Eq. (26) with respect to the jth design variable

$$[B]\frac{\partial\{X\}}{\partial d_j} + \frac{\partial[B]}{\partial d_j}\{X\} = 0 \tag{29}$$

Premultiplying by $\{v\}^T$ and using Eq. (26), one obtains

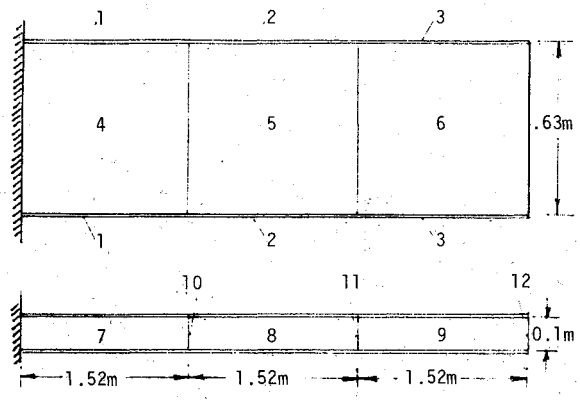

Fig. 3 Finite element model of wing box cantilever structure. Numbers indicate design variable ID nos. Symmetry ensures fixed chordwise location of the center of mass.

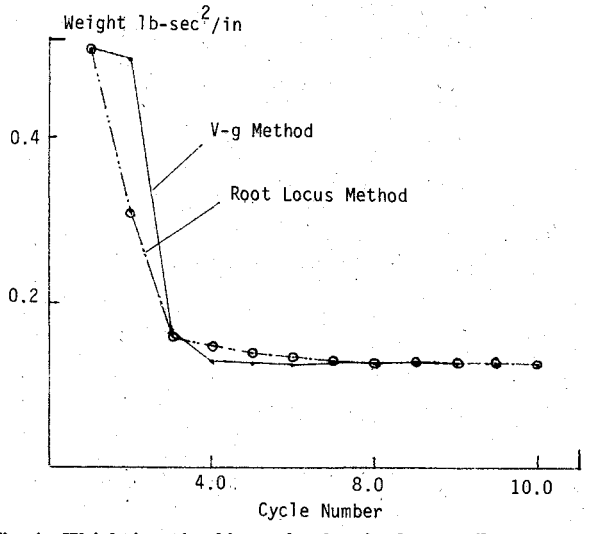

Fig. 4 Weight iteration history for the wing box cantilever structure.

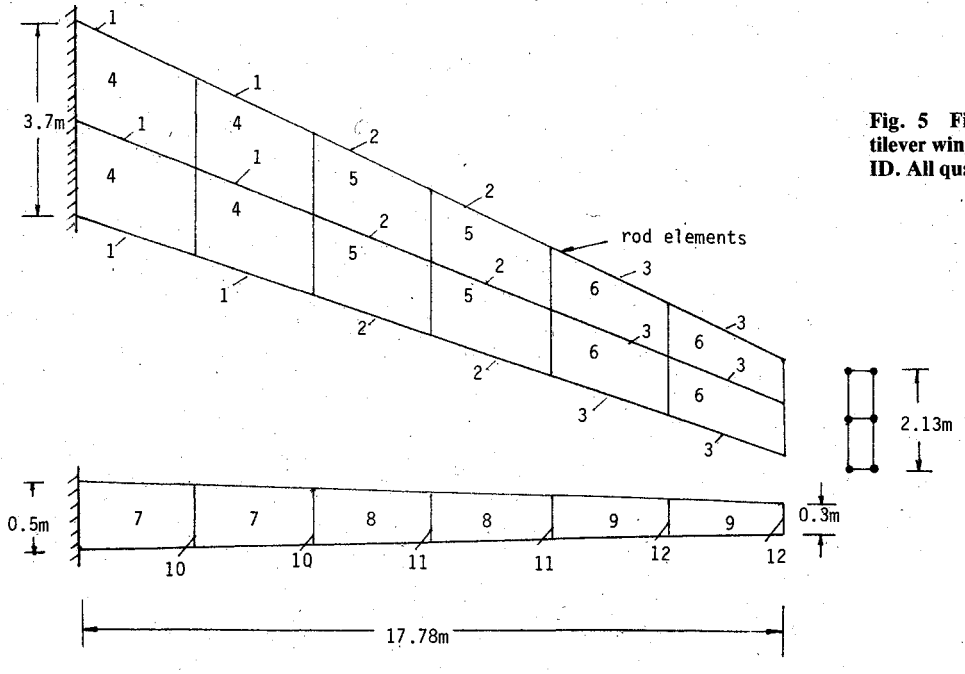

Fig. 5 Finite element model for the swept cantilever wing structure. Numbers indicate the element ID. All quadrilateral panels are membrane elements.

$$\{v\}^T \frac{\partial [B]}{\partial d_j} \{X\} = 0 \tag{30}$$

which can be written in the expanded form as

$$\{v\}^T \left(\bar{s}^2 \frac{\partial [\hat{M}]}{\partial d_j} + 2\bar{s} \frac{\partial \bar{s}}{\partial d_j} [\hat{M}] + \frac{\partial [\hat{K}]}{\partial d_j} - q \frac{\partial [\hat{A}]}{\partial \bar{s}} \frac{\partial \bar{s}}{\partial d_j} \right) \{X\} = 0 \tag{31}$$

For the chosen finite-element representation used in this exercise, the design variables are the thickness of membrane elements and cross-sectional areas of the bar elements. The mass and stiffness matrices are linear in these design variables and the sensitivity of these matrices can be obtained routinely in a finite-element program.[14] In an appendix of Ref. 7, the aerodynamics matrix is shown to have the following form

$$[\hat{A}(\bar{s})] = [\hat{A}]_0 + \bar{s}[\hat{A}]_1 + \bar{s}^2 [\hat{A}]_2 + C(\bar{s}) [\hat{A}]_3 + \bar{s} C(\bar{s}) [\hat{A}]_4 \tag{32}$$

Note that in Eq. (31) the derivative of the aerodynamics matrix with respect to the design variable d_j is zero. This stems from a constant mode assumption used in this exercise whereby the natural modes of vibration are assumed unchanged over a prescribed number of design iterations. The coefficient matrices $[\hat{A}]_i$ in Eq. (33) are constant matrices under this assumption.

The derivative of the aerodynamics matrix can be expressed as

$$\frac{\partial [\hat{A}(\bar{s})]}{\partial \bar{s}} = [\hat{A}]_1 + 2\bar{s}[\hat{A}]_2 + \frac{\partial C(\bar{s})}{\partial \bar{s}} [\hat{A}]_3 + \bar{s} \frac{\partial C(\bar{s})}{\partial \bar{s}} [\hat{A}]_4 + C(\bar{s}) [\hat{A}]_4 \tag{33}$$

Since the eigenvectors of the system are in general complex, the following definitions are used for ease of notation.

$$\{v\}^T \frac{\partial [\hat{M}]}{\partial d_j} \{X\} = DM \tag{34}$$

$$\{v\}^T \frac{\partial [\hat{K}]}{\partial d_j} \{X\} = DK \tag{35}$$

$$\{v\}^T \frac{\partial [\hat{A}]}{\partial \bar{s}} \{X\} = DA \tag{36}$$

$$\{v\}^T [\hat{M}] \{X\} = RM \tag{37}$$

where DM, DK, DA, and RM are, in general, complex scalar quantities. With these definitions, the derivative of $\bar{s}$ for each of the j design variables can be written as

$$\frac{\partial \bar{s}}{\partial d_j} = -\left(\frac{DK + \bar{s}^2 DM}{2\bar{s} RM - qDA} \right) \tag{38}$$

The real and imaginary parts of this expression can be used in the constraint formulations of Eqs. (13) and (20)-(23) as follows.

1) Aeroelastic stability constraint without damping considerations:

$$\frac{\partial g_i}{\partial d_j} = \frac{\partial \eta_i}{\partial d_j} = Re\left(\frac{\partial s_i}{\partial d_j} \right) \tag{39}$$

2) Aeroelastic stability constraint with prescribed viscous damping and response frequency:

$$\frac{\partial X_s}{\partial d_j} = \frac{1}{\gamma_{\text{ref}}} \frac{\partial \gamma}{\partial d_j} \tag{40}$$

$$\frac{\partial \gamma}{\partial d_j} = \frac{\partial \gamma}{\partial \eta} Re\left(\frac{\partial s_i}{\partial d_j} \right) + \frac{\partial \gamma}{\partial \tau} Im\left(\frac{\partial s_i}{\partial d_j} \right) \tag{41}$$

$$\frac{\partial Y_s}{\partial d_j} = \frac{1}{\omega_{\text{ref}}} \frac{\partial \omega_d}{\partial d_j} \tag{42}$$

$$\frac{\partial \omega_d}{\partial d_j} = \frac{\partial \omega_d}{\partial \eta} Re\left(\frac{\partial s}{\partial d_j} \right) + \frac{\partial \omega_d}{\partial \tau} Im\left(\frac{\partial s}{\partial d_j} \right) \tag{43}$$

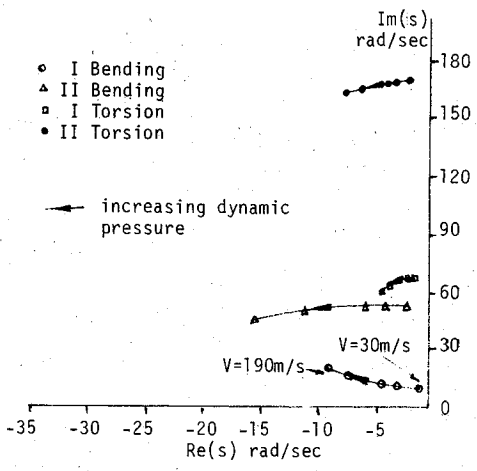

Fig. 6 Root locus plot at first iteration for swept wing.

Table 1 Comparison of results of flutter optimization using the *V-g* and the root locus procedures for stability analysis (The structure optimized for minimum weight is the primary structural box of an unswept cantilever wing.)

Element ID No.	Element type	Initial design	Final design *V-g* approach	Final design root locus method
1	AR[a]	12.9 cm^2	2.148 cm^2	2.148 cm^2
2	AR	12.9 cm^2	2.148 cm^2	2.148 cm^2
3	AR	12.9 cm^2	2.148 cm^2	2.148 cm^2
4	QM[b]	0.1015 cm	0.0411 cm	0.0387 cm
5	QM	0.1015 cm	0.0392 cm	0.0393 cm
6	QM	0.1015 cm	0.0348 cm	0.0363 cm
7	QM	0.203 cm	0.1485 cm	0.1387 cm
8	QM	0.203 cm	0.1399 cm	0.1405 cm
9	QM	0.203 cm	0.1348 cm	0.1387 cm
10	QM	0.1015 cm	0.0960 cm	0.0930 cm
11	QM	0.1015 cm	0.0960 cm	0.0930 cm
12	QM	0.1015 cm	0.0929 cm	0.0931 cm

[a] AR = axial road; [b] QM = quadrilateral membrane.

For purposes of computational efficiency, it is not desirable to update the natural modes of vibration for every iteration of the optimization process. However, the accuracy of the analysis begins to deteriorate with changes in the design variable vector. The natural modes of vibration were updated only after every five iterations. In the present work, a linear updating of the system stiffness and mass matrices was used to save on computational resources.

Table 2 Initial and final designs for the swept wing sized for a flutter constraint (Root locus approach used for flutter speed calculation.)

Element ID No.	Element type	Initial design	Final design
1	AR[a]	12.9 cm^2	3.226 cm^2
2	AR	12.9 cm^2	3.226 cm^2
3	AR	12.9 cm^2	3.226 cm^2
4	AR	0.1015 cm	0.0330 cm
5	QM[b]	0.1015 cm	0.0416 cm
6	QM	0.1015 cm	0.0502 cm
7	QM	0.203 cm	0.1424 cm
8	QM	0.203 cm	0.1597 cm
9	QM	0.203 cm	0.1779 cm
10	QM	0.1015 cm	0.0965 cm
11	QM	0.1015 cm	0.0987 cm
12	QM	0.1015 cm	0.1003 cm

[a]AR = axial road; [b]QM = guadrilateral membrane.

Table 3 Initial and final designs for the swept wing sized for a flutter constraint (Root locus approach used with prescribed stability margin.)

Element ID No.	Element type	Initial design	Final design
1	AR[a]	12.9 cm^2	5.101 cm^2
2	AR	12.9 cm^2	4.908 cm^2
3	AR	12.9 cm^2	3.904 cm^2
4	QM	0.1015 cm	0.0705 cm
5	QM	0.1015 cm	0.0391 cm
6	QM	0.1015 cm	0.0524 cm
7	QM	0.203 cm	0.1534 cm
8	QM	0.203 cm	0.1505 cm
9	QM	0.203 cm	0.1665 cm
10	QM	0.1015 cm	0.0961 cm
11	QM	0.1015 cm	0.0984 cm
12	QM	0.1015 cm	0.0996 cm

[a]AR = axial road; [b]QM = guadrilateral membrane.

$$[K] = [K]^{\text{old}} + \sum_{j=1}^{n} \frac{\partial [K]}{\partial d_j} \Delta d_j \tag{44}$$

$$[M] = [M]^{\text{old}} + \sum_{j=1}^{n} \frac{\partial [M]}{\partial d_j} \Delta d_j \tag{45}$$

Implementation

A finite-element analysis routine was coupled to an unsteady aerodynamics code and a feasible usable search direction optimizer CONMIN,[15] via pre- and postprocessors. All computations were performed on a VAX 11-780 system with the flow between the processors controlled in the DEC command language.

Test Examples

The unswept cantilever wing box model (Fig. 3) was used as the first test example to validate the synthesis procedure. The results of this exercise are presented in Table 1. There is good agreement between the results obtained through this approach and those from the *V*-g formulation. The weight iteration history for this example is depicted in Fig. 4 and shows a smooth convergence to the optimum.

A swept cantilever wing model was used as the second example in the method evaluation. This structure has 108

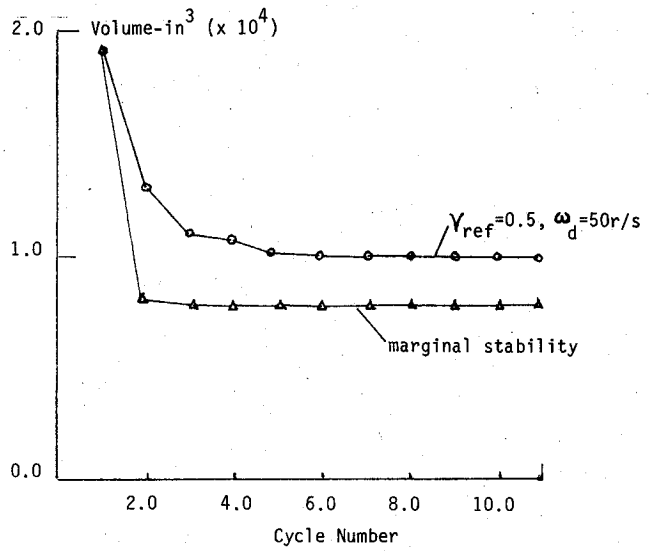

Fig. 8 Weight iteration history for the swept wing.

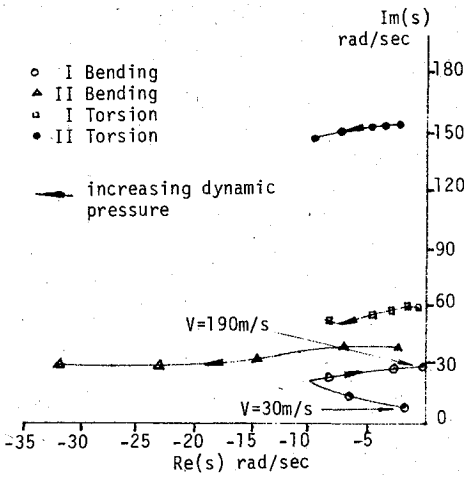

Fig. 7 Root locus plot at twelfth iteration for swept wing. Structure designed for marginal stability.

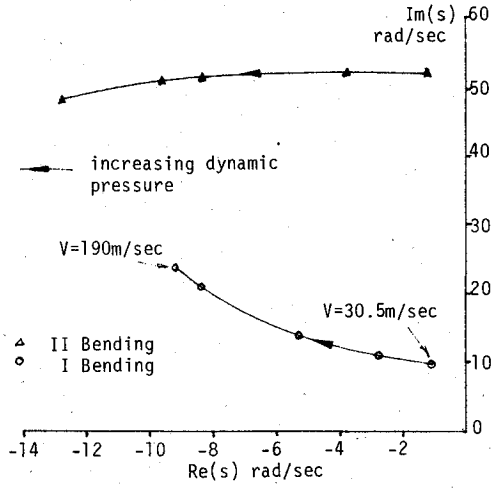

Fig. 9 Root locus at first iteration for the swept wing. Constraints on damped frequency and available viscous damping included.

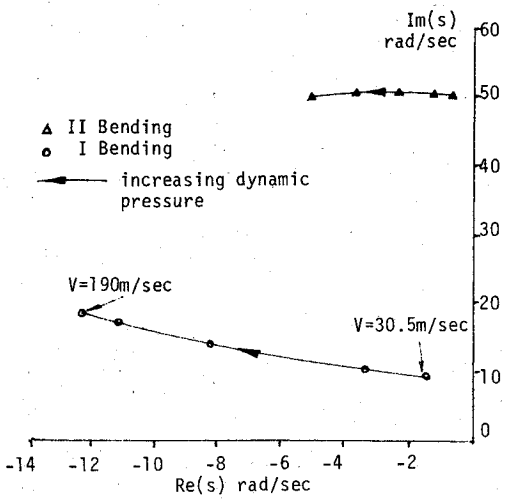

Fig. 10 Root locus plot at tenth iteration for the swept wing. Constraint on damped frequency and available damping included.

degrees of freedom. The finite-element model of its primary structural box is depicted in Fig. 5. The membrane and rod model was once again reduced to a twelve design variable problem. Five natural modes of vibration, three primarily bending and two torsion, were used to model the deformation of the structure. For each of the 10 dynamic pressures, 20 roots had to be monitored for stability, a choice which resulted in 200 inequality constraints. The design task was to insure flutter-free performance for speeds up to 190 m/s. The marginal stability requirements of Eq. (13) were used. The initial and final designs for the problem are presented in Table 2. Figures 6 and 7 show the root locus plots for the first and twelfth iterations of the design process. The weight iteration history is shown in Fig. 8. There is a rapid convergence to the optimum, with most of the excess weight eliminated in the first five iterations.

The swept cantilever wing model was also sized for a constraint on the damping ratio and the frequency of the response. In addition to the constraints on marginal stability from the previous exercise, for flight speeds of 160, 175, and 190 m/s, additional constraints are imposed by prescribing $\gamma_{ref} = 0.5$ and $\omega_{ref} = 50$ rad/s. This results in a total of 260 inequality constraints to be represented by the single cumulative measure. Root locus plots for the first and tenth iterations are shown in Figs. 9 and 10. The volume convergence history is illustrated in Fig. 8. As would be expected, the additional constraint results in a higher weight. The initial and final designs for this example are shown in Table 3.

Conclusions

The problem of optimal design for flutter considerations is examined from the viewpoint of a gradient-based nonlinear programming approach. Formulation of a flutter constraint that does not require an actual computation of the flutter speed results in a very large number of inequality constraints. The cumulative constraint representation permits the formulation of an efficient generalized constraint that circumvents this problem without having to resort to penalty function-based unconstrained minimization techniques. The generalized constraint can be used in conjunction with a widely used *V-g* method of flutter analysis. The inherent problems in this method, however, suggest the use of an alternative analysis technique and the root locus approach is proposed as a viable choice. This approach is preferable as it permits the user to conduct the aeroelastic stability analysis for only those flight conditions that are of interest by an appropriate choice of the dynamic pressure parameter. It also allows the formulation of a constraint wherein safety margins can be prescribed in the optimized design. The gradients of the flutter constraint with respect to sizing variables can be computed analytically. The design strategy has been validated for representative structural models.

Acknowledgment

This research was supported under Grant NGL 05-020-243 from the NASA Langley Research Center.

References

[1] Turner, M.J., "Optimization of Structures to Satisfy Flutter Requirements," *AIAA Journal,* Vol. 7, May 1969, pp. 945-951.

[2] McIntosh, S.C., "Structural Optimization Via Optimal Control Techniques: A Review," Structural Optimization Symposium, AMD-Vol. 7, 1974.

[3] Stroud, W.J., "Automated Structural Design with Aeroelastic Constraints: A Review and Assessment of the State of the Art," Structural Optimization Symposium, AMD-Vol. 7, 1974.

[4] O'Connell, R.F., Hassig, H.J., and Radovich, N.A., "Study of Flutter Related Computational Procedures for Minimum Weight Structural Sizing of Advanced Aircraft," NASA CR-2607, March 1976.

[5] Bisplinghoff, R.L. and Ashley, H., *Principles of Aeroelasticity,* Dover Publications, New York, 1975, pp. 235-240.

[6] Hajela, P., "Further Developments in the Controlled Growth Approach for Optimal Structural Synthesis," ASME Paper DET 82-058, presented at 12th Design Automation Conference, Arlington, Va., Sept. 1982.

[7] Hajela, P., "Techniques in Optimum Structural Synthesis with Static and Dynamic Constraints," Ph. D. Thesis, Stanford University, July 1982.

[8] Bisplinghoff, R.L., Ashley, H., and Halfman, R.L., *Aeroelasticity,* Addison-Wesley Publishing Co., Mass., 1955, pp. 555-590.

[9] Greene, W.H. and Sobieski, J.S., "Minimum Mass Sizing of a Large Low Aspect Ratio Airframe for Flutter Free Performance," NASA TM-81818, May 1980.

[10] Yates, E.C., Jr., "Modified-Strip-Analysis Method for Predicting Wing Flutter at Subsonic to Hypersonic Speeds," *AIAA Journal,* Vol. 3, Jan-Feb. 1966, pp. 124-128.

[11] Jones, R.T., "Operational Treatment of the Nonuniform Lift Theory to Airplane Dynamics," NACA TN 667, 1938.

[12] Edwards, J.W., "Unsteady Aerodynamic Modelling and Active Aeroelastic Control," SUDAAR 504, Stanford University, Feb. 1977.

[13] Gwin, L.B. and Taylor, R.F., "A General Method for Flutter Optimization," *AIAA Journal,* Vol. 11, Dec. 1973, pp. 1613-1617.

[14] Rogers, J.L., Jr., Sobieski, J.S., and Bhat, R.B., "An Implementation of the Programming Structural Synthesis System (PROSSS)," NASA TM-83180, Dec. 1981.

[15] Vanderplaats, G.N., "CONMIN—A Fortran Program for Constrained Function Minimization," NASA TMX-62282, 1973.